European Association for the Development of Renewable Energies, Environment and Power Quality (EA4EPQ)

International Conference on Renewable Energies and Power Quality (ICREPQ'10)
Granada (Spain), 23rd to 25th March, 2010

Modelling and Optimization of a Concentrating PV-Mirror System

I. S. Hermenean[1], I. Visa[1] A. Duta[1] and D. V. Diaconescu[1]

[1] Department of Product Design for Sustainable Development
Transilvania University Brasov
B-ul Eroilor, 29, 500036 Brasov (Romania)

Phone/Fax number: +40-(268) 41.20.88, +40-(268) 41.05.25, e-mail: **ioana.hermenean@unitbv.ro**

Abstract. The paper presents results on a novel low concentration system for photovoltaic/ hybrid module, its geometric modelling and the optimal working parameters. The low concentration system is build up of a PV module and two mirrors, one on the left side and symmetrically on the right side along the length of the PV module. Our objective is to maximize the received direct radiation of the PV or hybrid module, maintaining an overall geometric size of the system as small as possible with a minimum number of the tracking steps. Two cases were considered: the first case when the reflected solar radiation from each mirror sweeps the whole surface of the PV module increasing by almost 2x the amount of radiation that sweeps the PV-surface; the second case when the reflected light from each mirror partially sweeps the PV-module surface, building together one cover of light on the plane and increasing the amount of radiation that falls on the module surface around 1x. Although the total amount of radiation that falls on the photovoltaic/hybrid module surface in the second case is far less than in the first situation, the overall size of the system is strongly reduced.

Key words

Low solar concentrator, photovoltaic/hybrid modules, mirrors, tracking efficiency.

1. Introduction

The concentrating solar systems (CPV) use reflective and refractive optical devices to focus the solar light onto a photovoltaic surface and so to increase the energetic output. The aim of such a system is to increase the power output by reducing the expensive PV surface, using low cost optical materials and parts. The most important aspect of this technology is the possibility to reach system efficiencies beyond 30% [1]. There are three main types of concentrating systems, with low, medium and high concentrating ratio. One limitation of the medium- and high-concentration systems is the requirement for highly accurate tracking for maintaining the focus of the light on the solar cells as the sun moves throughout the day, adding extra costs and complexity to the system. Due to the simple geometry of the low concentrating photovoltaic or hybrid systems the tracking precision required is not so high.

This paper relates to a low concentration system; it presents the geometric modelling followed by the analysis of the main parameters with influence on the amount of the input radiation amount.

The simulations were developed considering the equatorial tracking system for the geographical location of the Brasov - Romania area, using specific regional parameters, considering the ideal meteorological conditions.

The solar radiation data registered in the past four years, by the Transilvania University Brasov Meteorological station, shows a significant amount of diffuse radiation, therefore the low concentration system is build up of a PV module and two mirrors, symmetrically disposed on the left and right side along the length of the PV module, as presented in Fig.1.

For non concentrated PV systems: $TotalRadiation = DirectRadiation + DiffuseRadiation$,

while for the Low CPV system discussed in this paper: $TotalRadiation = x \cdot DirectRadiation + DiffuseRadiation$,

where x is the concentration ratio, defined as the ratio between the received quantity of radiation on the PV-module and the available Radiation quantity. [2]

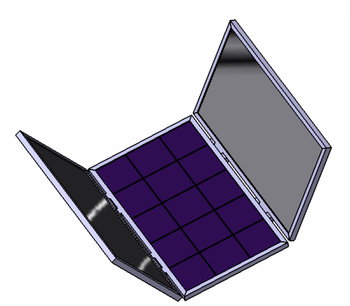

Fig.1. Low solar concentrating system build up by a photovoltaic or hybrid module and two laterally disposed mirrors

Our objective is to maximize the global direct radiation incident on the PV module (or hybrid) while maintaining an overall geometric size of the system and the tracking steps at minimum values. Through numerical simulations the parameters that influence functionality of the assembly can be identified, making optimization possible.

2. Geometric Modelling

The geometric modelling starts from the system in Fig. 1 which is equatorial (polar) tracked. Based on the basic geometric model of the low CPV system we consider two cases: (1) when the reflected solar radiation from each mirror sweeps the entire surface of the PV module (or hybrid), assuring a double coverage with reflected light (Fig. 2 a, Fig. 3a) and (2) when the reflected light from each mirror partially sweeps the PV-module (or hybrid) surface, building together a single light cover on the PV plane (Fig. 2 b, Fig. 3b).

The main geometric parameters of the model are: the inclination angle between the PV-module and the mirror (θ), the ratio L1/ L2 (ε) , the incidence angle [3], υ_M – maximum incidence angle (when positioned to the right, $\upsilon_M > 0$), υ_m- minimum incidence angle (when positioned to the left, $\upsilon_m = -\upsilon_M$ see Fig.2), υ_{M11}, υ_{M12}, υ_{M13} – incidence angle reflected by the right mirror, M1 on the PV module, right extreme, median and left extreme and analogue υ_{M21}, υ_{M22}, υ_{M23} for the left mirror, M2. For the angle υ_M we considered the values υ_M= 15°, 7.5, 3.75°, 1,875°, knowing that the sun moves with ~15°/hour.

The angular displacement of the tracked CPV system is made discontinuously (in steps), so the tracker's equatorial angles (hour angle and declination angle) have discreet variations [4].

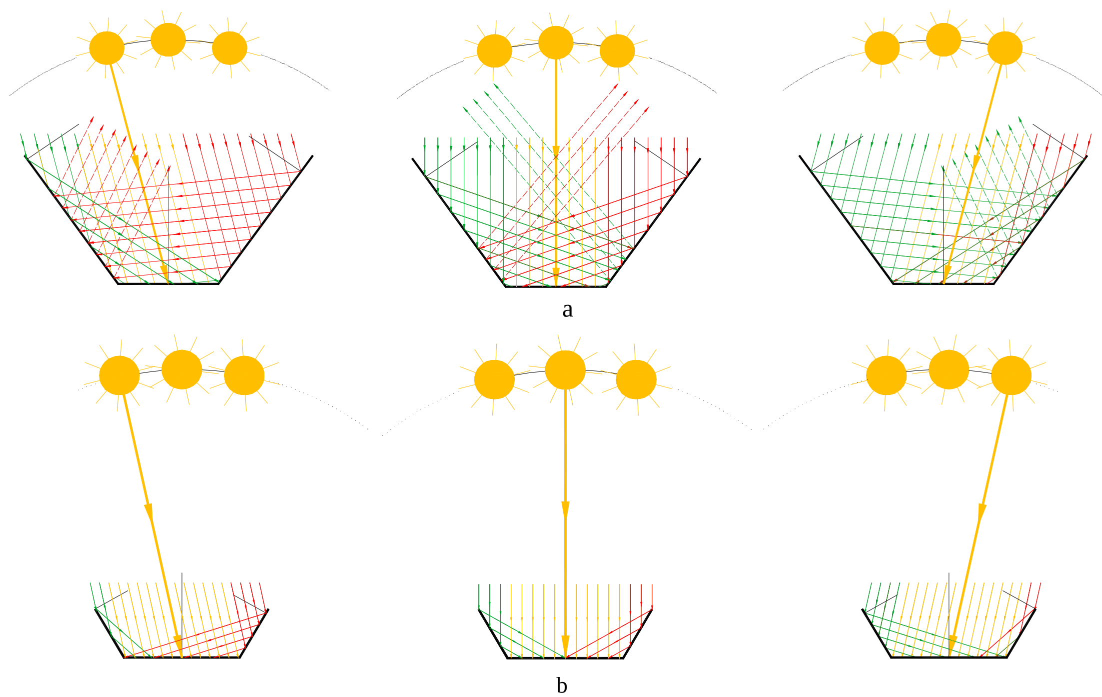

Fig.2. Low Concentrating System Model during one step interval: a) first case, b) second case.

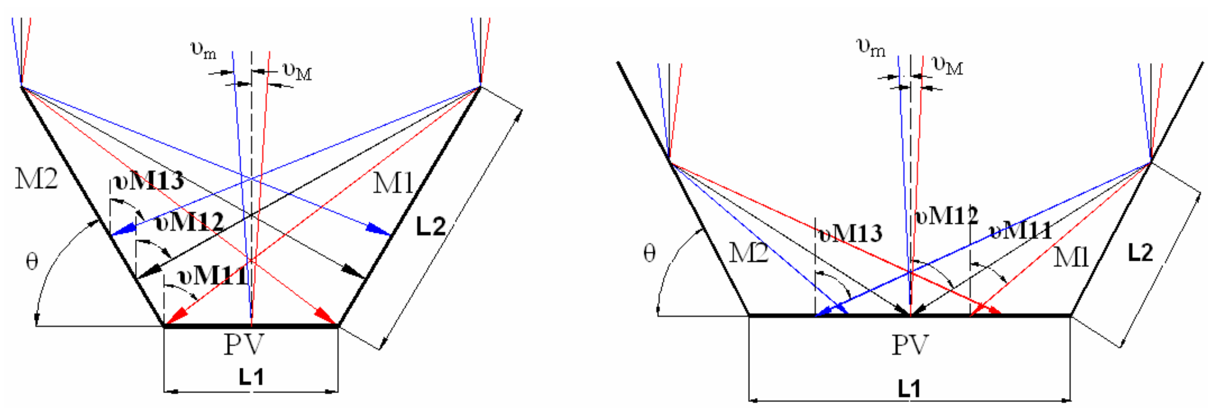

a b

Fig.3. Low solar concentrating models with the length of the mirror the same with the PV module length: a) first case; b) second case.

A step interval is build up by the rotation time (~ 1s) and rest time till the next rotaion. The declination angle is considered constant during o day, due to it's low varaition during a day light period (0.17°/day). The system during one step interval, for the first case can be seen in Fig. 2a and respecivly for the second case in Fig. 2b.
For the case of equatorial tracking system, for the above mentioned values of υ_M corresponds the following time intervals: υ_M= 15° ⇔ 2h , υ_M= 7.5°⇔1h, υ_M= 3.75° ⇔ 30min and υ_M= 1,875° ⇔ 15min.
To further determine the geometric parameters and so the dimensions of the CPV system, Fig. 4 was used.

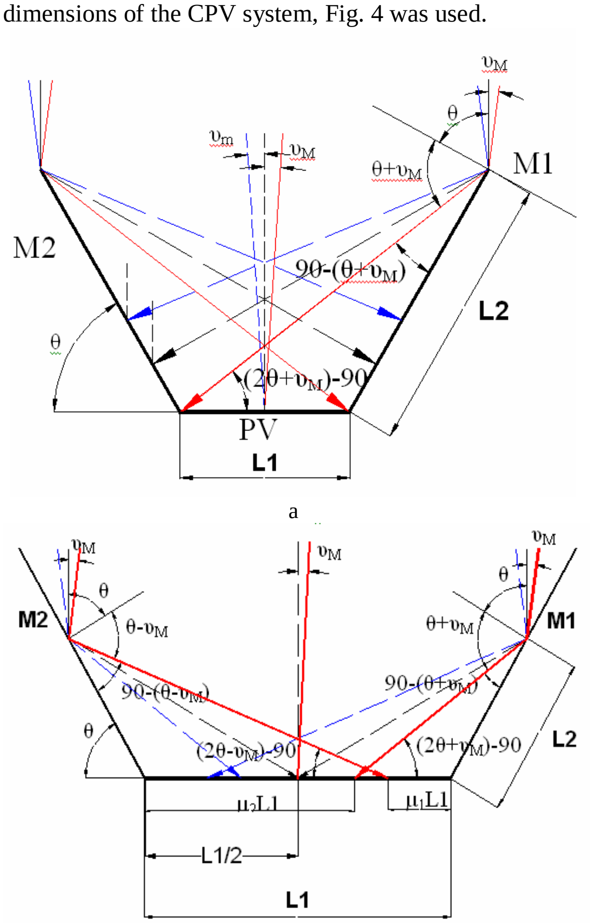

b

Fig.4. Geometric model used for the dimensioning of the CPV system: a) first case and b) second case.

In the first case, a large concentration ratio was observed, consequently, a large overall size of the system. This depends on the L1 and L2 values of the system. Considering fixed the width of the photovoltaic/ hybrid module (L1), the width of the mirror (L2) can be evaluated, respecting the condition of light reflectance on the entire surface of the module, see Fig. 4a.
While in the second case our goal is to reduce the surface of the mirror, thus to reduce the overall size of the system, by stating that the solar radiation falling from each mirror sweeps about half of the PV surface, see Fig. 2b and 3b. In this case we start with knowing the length of the PV, L1; considering that the solar ray covers L1/2, we determine the value of L2, length of the mirror.
Based on Fig. 4, the ratio between L1 and L2 was calculated: ε1 for case one and ε2 for the second case:

$$\varepsilon 1 = \frac{L2}{L1} = \frac{-\cos(2\cdot\theta + \upsilon_M)}{\cos(\theta + \upsilon_M)} \tag{1}$$

$$\varepsilon 2 = \frac{L2}{L1} = \frac{-\cos(2\cdot\theta)}{\cos(\theta)} \tag{1'}$$

Expression (1) was determined based on the position of the extreme sun ray, Fig. 4a - red colour, depending on the maximum incidence angle, while (1') considers the sunray that falls in the middle of the PV-module, Fig. 4b-black colour.
Based on these expressions, the curve family presented in Fig. 5 is developed, which shows that the width of the mirror increases, due to θ angle, with the incidence angle.

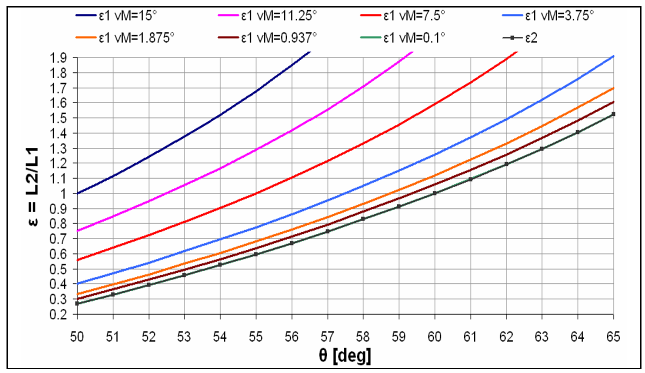

Fig. 5. Variations of ε1 and ε2

For the second case, the variation of ε2 is almost equal to the variation of ε1 during a low incidence angle which means an accurate tracking.
With the value of L2, for different values of θ, we can determine the position of the sunray on the PV-module; two coefficients are introduced: μ_1, for the reflected light from mirror M1, and μ_2 for M2. These coefficients multiplied with the length of the PV-module (L1) allow the calculation of the PV-module surface that is swiped by the reflected light.
Based on the Fig. 4b we can write:

$$\mu_1 = \frac{L2\cdot\cos(\theta + \upsilon_M)}{-L1\cdot\cos(2\cdot\theta + \upsilon_M)} \tag{2}$$

$$\mu_2 = \frac{L2\cdot\cos(\theta - \upsilon_M)}{-L1\cdot\cos(2\cdot\theta - \upsilon_M)} \tag{2'}$$

The diagrams in Fig. 6 show the variation of the coefficients μ, in percent, for different values of the inclination angle θ; it can be seen that the optimal values of μ can be achieved at low values of υ_M. These diagrams also show that the optimum inclination angle for the mirrors is θ = 65°.
The next subchapter presents a comparative analysis based on numerical simulations.

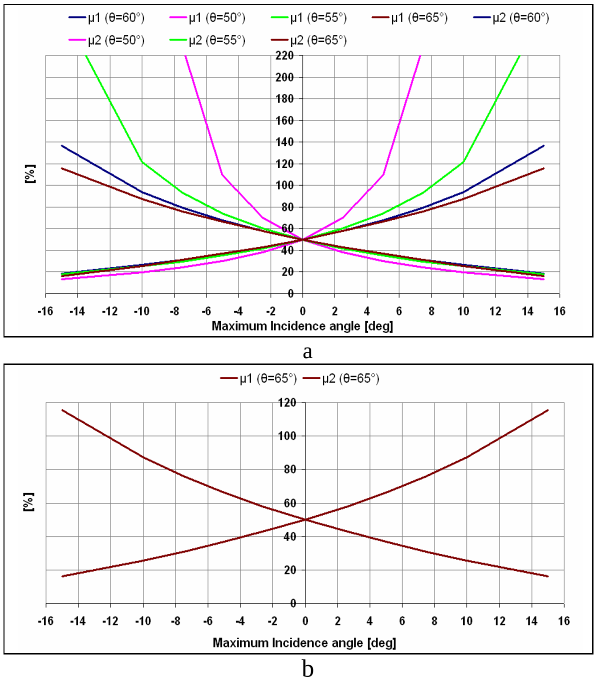

Fig.6. Variation of the μ coefficient vs the maximum incidence angle ν_M, for : a) different values of angle θ and b) θ = 65°.

3. Influence Analysis of the Geometric Parameters by Numerical Simulations.

The main objective is to determine the increase in the radiation amount that falls on the PV-module, due to the reflected component from the mirrors. The direct radiation on the PV-module surface, provided by the two mirrors has different values due to the different incidence angles between reflected rays and PV module. In the analysis is considered that this fact does not influence the proper functioning of the PV module. Also as a primary assumption we consider that nothing is lost through reflection from the radiation that falls on the mirror, ignoring in this stage the multiple reflections.

The corresponding numerical simulations are developed considering the Brasov/Romania location (with the latitude φ = 45.6ºN and the turbidity factor T_R=3), during the summer solstice (N = 172 and δ = + 23.5º) and using an equatorial tracking.

The parameters used are: the θ angle (50°, 55°, 60°, 65°), different incidence angle values (υ_M= 15°, 7.5, 3.75°, 1,875°), considering L1= 500mm and μ1,2 for the second case.

The amount of direct solar Radiation is computed with the equations [5]:

$$B_S = B_0 \exp\left[-T_R/(0.9 + 9.4\sin\alpha)\right] \quad (3)$$

$$B_0 = 1367 \cdot \left[1 + 0.0334 \cdot \cos(0.9856 \cdot N - 2.27\right] \quad (3')$$

Where Bs is the direct solar Radiation, T_R is the turbidity factor [5], α is the altitude angle and N – day number in a year.

The radiation that falls normal on the PV, due to the sun ray reflection on the mirrors, is computed by means of the Lambert Law, as follows:

- For the first case:

$$B_{pv_{M1,2}} = B_s \cos(\nu_{M1,2}) \quad (4)$$

- For the second case:

$$B_{pv_{M1,2}} = \mu_{1,2} B_s \cos(\nu_{M1,2}) \quad (4')$$

The expression (4') gives the average equivalent radiation that falls normal on the whole PV-module from reflected rays of each mirror. The variation of the radiation $B_{pvM1,2}$ is presented in Fig. 7 for the first case and in Fig. 8 for second case.

The diagrams represent the variations of the solar radiation that falls normal on the PV module surface, at different tracking steps and the extreme values of θ (50°and 65°), considering both cases.

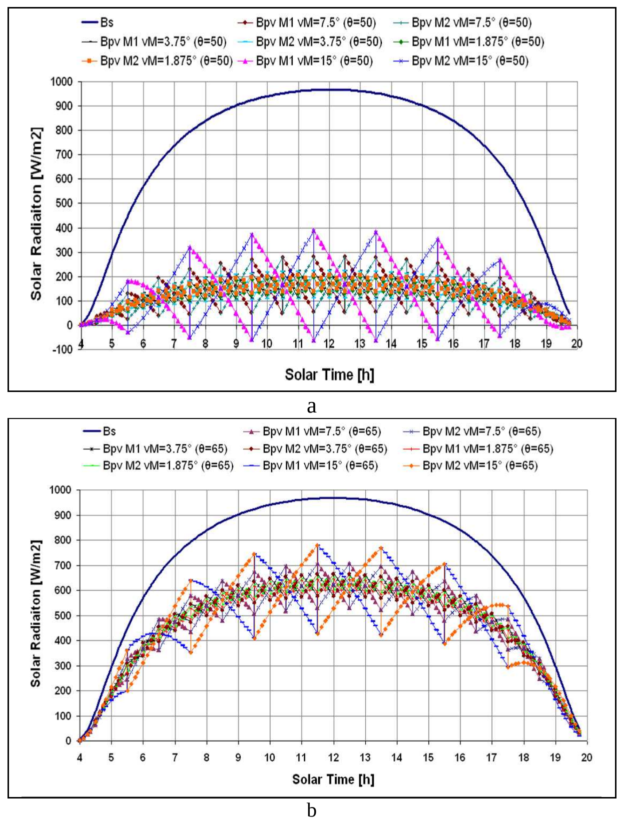

Fig.7. First case: Variations of the direct solar radiation normal on PV from each of the two mirrors, at different θ and υ_M values, compared with the available direct radiation: a) θ= 50°, b) θ= 65°.

The total radiation that falls on the PV as reflection from the mirrors is the sum between the radiation from mirror one and respectively mirror two.

$$B_{pv_M} = \sum B_{pv_{M1,2}} \quad (5)$$

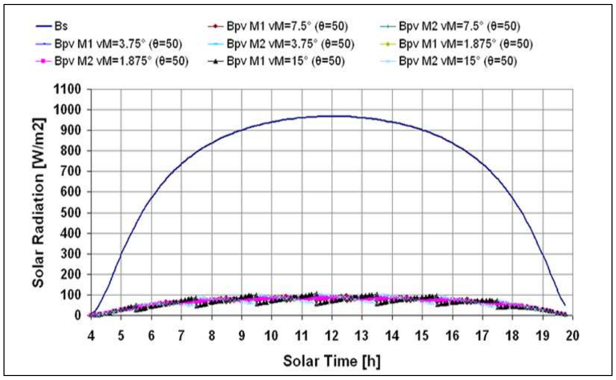

a

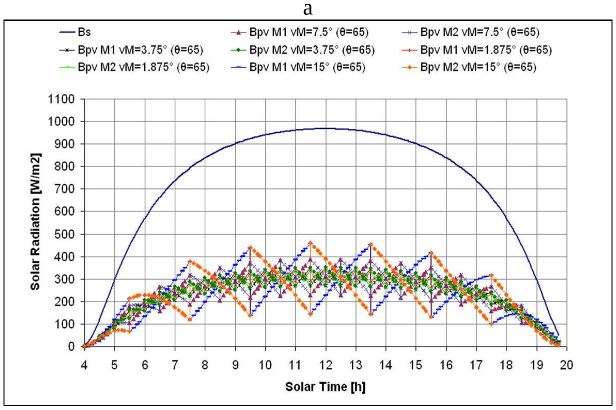

b

Fig.8. Second case: Variations of the direct solar radiation normal on PV from each of the two mirrors, at different θ and υ_M values, compared with the available direct radiation: a) θ= 50°, b) θ= 65°.

a

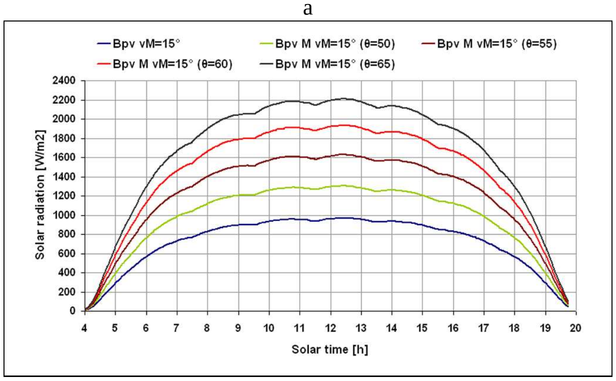

b

Fig.9. First case: Variations of total direct radiation normal on PV, at different θ values, compared with the PV direct radiation without mirrors, at different values of υ_M: a) υ_M= 1,875° and b) υ_M= 15°.

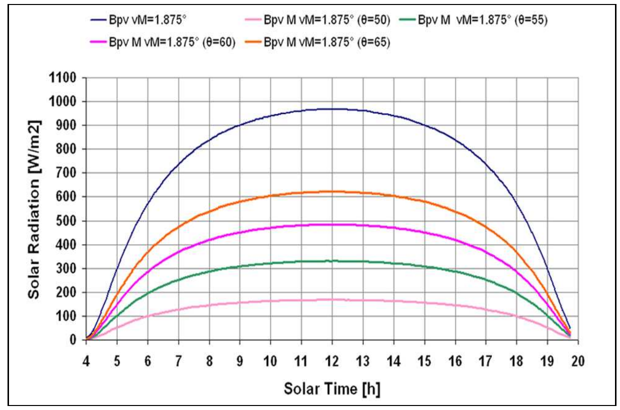

a

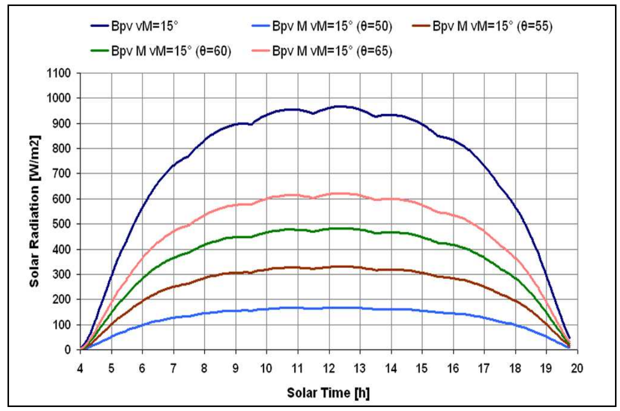

b

Fig.10. Second case: Variations of total direct radiation normal on PV, at different θ values, compared with the PV direct radiation without mirrors, at different values of υ_M : a) υ_M= 1,875° and b) υ_M= 15°.

The diagrams in Fig. 9 and Fig.10 represent the total solar radiation variation from both mirrors and the direct radiation that falls normal on the PV module, at different values of the angle θ and at extreme values of υ_M (1,875°, 15°), in both discussed case.

The diagrams in Fig.10 represent the total solar direct radiation that falls normal on the PV module in two extreme orientation cases: tracking step duration of 2 h and respectively of 15 min), due to the fact that the total radiation dose not depend on the tracking step interval.

The diagrams in Fig.10 show the variations of different radiations: the direct radiation that falls normal on a fix tilted PV module, the direct radiation that falls normal on the equatorial tracked PV module and the total direct radiation falls normal on the PV module from the CPV system: the sum between the direct radiation derived from reflected radiation of two mirrors and from one that falls direct on the PV module. The concentration ratio in the first case is ~1.3-2.2x, depending only on θ. For large θ values, the ratio increases as well as the overall size of the system, (Fig.10a). In the second case, where the aim is to reduce the overall size of the concentrating system by using smaller mirrors, while maintaining a high amount of incident solar radiation, the increase of the absolute efficiency of the system is with ~1.1-1.6x of the available solar radiation (Fig. 10b). The diagrams represent a comparison with the available radiation.

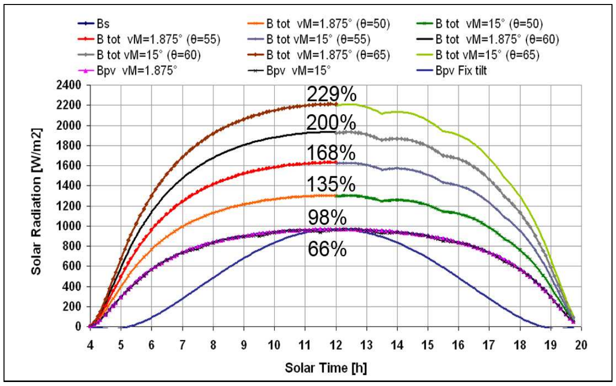

a

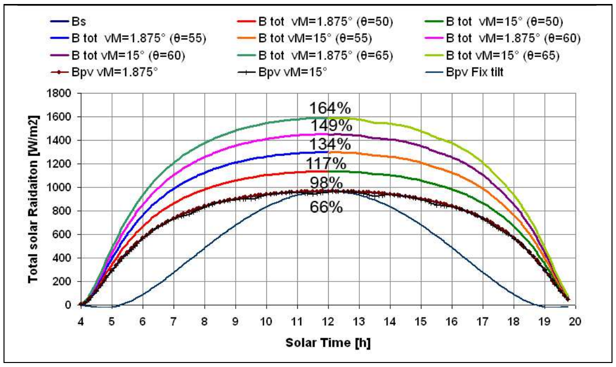

b

Fig.10. Total direct solar radiation variations that fall on the PV-module, at different values of angle θ and different values of maximum incidence angle ν_M: a) first case (Fig.3a) and b) second case (Fig.3b).

The numerical results emerged from analysis of Fig. 8-10 have been systematized in Table I.

Table I

θ [°]	Case	Absolute tracking efficiency*	Relative tracking efficiency 1**	Relative tracking efficiency 2***
50	1(Fig.3a)	135%	137%	205%
	2(Fig.3b)	117%	120%	177%
55	1(Fig.3a)	168%	171%	255%
	2(Fig.3b)	134%	137%	203%
60	1(Fig.3a)	200%	204%	303%
	2(Fig.3b)	149%	152%	226%
65	1(Fig.3a)	229%	234%	347%
	2(Fig.3b)	164%	167%	248%

* compared to the direct available radiation

** compared to the direct radiation that falls on the PV module without concentrators

*** compared to the direct radiation that falls on a fix tilted PV module without concentrators

4. Conclusion

The main paper conclusions regard the following aspects:

1) This paper presents a low concentrating system in two different cases: (1) when the reflected solar radiation from each mirror sweeps the entire surface of the PV module (or hybrid), assuring a double coverage with reflected light and (2) when the reflected light from each mirror sweeps partially the PV-module (or hybrid) surface, building together a single light cover on the PV plane.
2) The simulation was made neglecting some secondary effects and considering an equatorial tracking, the Brasov/Romania location, during the summer solstice.
3) The main geometric parameters of the model are: θ - angle between a mirror- and the PV plane, ε = L2/L1 - the ratio between the mirror width and the PV width, υ_M - maximum incidence angle (PV-sunray), μ_1 and μ_2 - the PV partial sweeping coefficients of the mirrors.
4) During the first case, ε1 depends on the θ angle as well as on the maximum incidence angle υ_M and it increases due to the θ and υ_M values; in the second case, ε2 depends only on the values of θ and not on υ_M.
5) The overall size in the first case (described by the ratio ε1) tends to overlap the overall size of the second case system (ε2) when the tracking accuracy increases; during continuous orientation of the first case system, the overall sizes of the two cases become equal.
6) The results show that the maximum values of tracking efficiency are obtained for high values of θ (in these cases 65°): 2.2x in the first case and 1.6x in the second case; because this means big overall sizes, a rational compromise must be made.
7) A reasonable compromise solution (with good efficiencies and acceptable overall sizes) is to use a system similar to the one in case 1 with high accurate tracking and mirror's angle θ contents in the range 55°-60°.
8) Another good compromise solution can be obtained by combining a low accurate tracking with a fine discreet adjustment of the mirror's angle θ.

Further research will focus on the tracking system accuracy, using different tracking programs and tracker types (equatorial, azimuth or pseudo-equatorial).

Acknowledgement

This paper is supported by the Sectoral Operational Programme Human Resources Development (SOP HRD), financed from the European Social Fund and by the Romanian Government under the contract number POSDRU/6/1.5/S/6".

References

[1] F.H. Klotz, "European Photovoltaic V-trough concentrator system with gravitational tracking (ARCHIMEDES)", Proceedings of the 16th European Photovoltaic Solar Energy Conference, Glasgow, UK, 1 - 4. May 2000, pp. 2229

[2] A. L. Luque, V. M. Andreev, Concentrator Photovoltaics, Springer-Verlag, Berlin Heidelberg, 2007.

[3] I.S. Hermenean, I.Visa, D.V. Diaconescu, On the Geometric Modelling of a Concentrating PV-Mirror System, Bulletin of the Transilvania University of Brasov, Vol. 1 (50) - 2009 • Series I, pp. 73-80

[4] I. Visa, D. Diaconescu, V. Popa, B. Burduhos, On the Incidence Angle Optimization of the Dual-Axis Solar Tracker, 11th International Research/Expert Conference TMT Hammamet, Tunisia, September 2007, pp. 1111-1114.

[5] M. Meliss, Regenerative Energie-quellen Praktikum, Springer, Berlin (1997), pp. 5-7.